Available online at www.sciencedirect.com

ScienceDirect

IFAC-PapersOnLine 48-19 (2015) 214–219

Stochastic Analysis of a 6-DOF Fully Parallel Robot under Uncertain Parameters ⋆

F.A. Lara-Molina and E. H. Koroishi * D. Dumur ** V. Steffen Jr. ***

* *Department of Mechanical Engineering, Federal Technological University of Paraná, Cornélio Procópio-PR, Brazil (e-mail: fabianmolina@utfpr.edu.br)*
** *Control Department, LSS - Centrale Supélec, Gif sur Yvette Cedex F-91192, France (e-mail: Didier.Dumur@centralesupelec.fr)*
*** *School of Mechanical Engineering, Federal University of Uberlândia, Uberlândia-MG, Brazil (e-mail: vsteffen@mecanica.ufu.br)*

Abstract: This paper aims at analyzing the effect of uncertain parameters on a 6-DOF fully parallel robot performance by using a stochastic approach. The uncertainties of the parameters are considered as small variations with respect to their nominal values modeled by means of random variables. The dynamics of the robot under uncertain structural and dynamic parameters including a computed torque position controller is analyzed. Additionally, a sensitivity analysis allows to determine the degree of influence of each uncertain parameter on the response of the robot. Numerical simulations illustrate the proposed methodology so that the effect of uncertain parameters on the dynamic performance of the robot is properly described.

Keywords: Robotic manipulators, Robot dynamics, Uncertainty, Sensitivity analysis, Random variables.

1. INTRODUCTION

Parallel robots are unavoidably subject to uncertainties. The main sources of uncertainties include various aspects such as manufacturing limitations and assembling tolerances of the mechanical parts, noise in the sensors, and unmodeled dynamics in the control system. Furthermore, in several applications, the robots operate with different values of payload to perform a specific task (e.g. pick and place robots).

Despite uncertainties, the parallel robots should be able to execute diverse tasks with high accuracy and repeatability which requires high reliability (e.g. robots used in medical applications). Therefore it is necessary to analyze the effects of uncertain parameters on the dynamic response in order to observe the behavior of the parallel robots under these conditions.

Several methodologies have been used to analyze uncertainties in robot manipulators. The stochastic approach has been widely applied to study the effects of uncertain parameters on the behavior of robot manipulators. In agreement with this approach, the effect of tolerances associated with the manipulator parameters on the reliability was studied (Kim et al., 2010; Pandey and Zhang, 2012). Moreover, Polynomial Chaos Theory was applied to study the effect of uncertain inertia and payload on SCARA robot dynamics (Voglewede et al., 2009).

Interval analysis has been also applied to study the uncertainties aiming at ensuring the reliability of robot manipulators (Merlet, 2009). Additionally, an approach based on fuzzy dynamic analysis has been applied to study uncertain parameters in a robot manipulator (Lara-Molina et al., 2014a). The aforementioned approaches are suitable when the stochastic process that governs the uncertainty is unknown; thus uncertain parameters are modeled by means of fuzzy variables.

According with the previous discussion, it is necessary to analyze the dynamic response of parallel robots under uncertain parameters, i.e., to analyze how the robot dynamics is affected by uncertain dynamic parameters, and thus to quantify these effects into the dynamic response of the robot by using straightforward numerical methods. Furthermore, it is necessary to evaluate the effect of uncertain parameters in terms of position accuracy of the parallel robots.

In this contribution the dynamics of a 6-DOF fully parallel robot with random uncertain parameters is analyzed. The simulation of the robot with uncertain parameters is performed by means of a numerical method based on the Monte Carlo simulation, hence, the position accuracy of the parallel robot controlled by PID-computed torque is analyzed under uncertain parameters. Additionally, the sensitivity in terms of the position accuracy of the un-

⋆ This work was supported by the National Institute of Science and Technology of Smart Structures in Engineering (INCT-EIE), jointly funded by CNPq, CAPES and FAPEMIG.

2405-8963
Peer review under responsibility of International Federation of Automatic Control.
10.1016/j.ifacol.2015.12.036

certain parameters is analyzed. This paper is organized in three sections. Section 2 introduces the robot manipulator model and the tracking position control scheme. In section 3, the stochastic uncertainty analysis is presented. Section 4 presents the sensitivity analysis. The numerical results are shown in section 5. Finally, the conclusions and further work are outlined.

2. ROBOT MODELING

The 6-UPS Stewart-Gough manipulator has six identical legs connecting the fixed base to the movable platform by universal joints denoted by U at points B_i and spherical joints denoted by S at points P_i (for $i = 1, \ldots, 6$), respectively. Both the universal and the spherical joints are passive. Each leg has an upper and a lower member connected by an active prismatic joint denoted by P that extends and retracts the leg. The movable platform has six degrees of freedom, three translational and three rotational motions. Fig. 1 shows the Stewart-Gough manipulator.

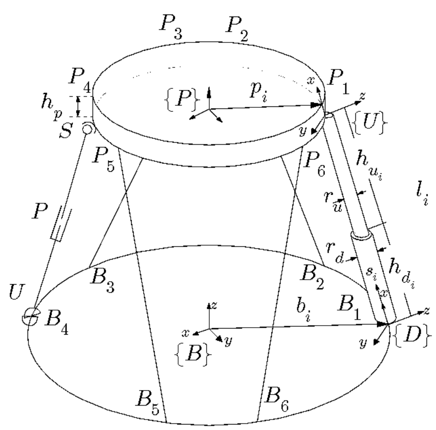

Fig. 1. Stewart-Gough robot.

2.1 Structural modeling

Two coordinate frames $\{P\}$ and $\{B\}$ are attached to the movable and fixed base respectively. The vector $\mathbf{b}_i = [b_{ix}\ b_{iy}\ b_{iz}]^T$ describes the position of the reference point B_i with respect to the frame $\{B\}$; In the same way, the vector $\mathbf{p}_i = [p_{ix}\ p_{iy}\ p_{iz}]^T$ describes the position of the reference point P_i with respect to the reference frame $\{P\}$ (see Fig. 2).

$$\begin{aligned} \mathbf{b}_i &= [r_b \cos(\psi_i)\ r_b \sin(\psi_i)\ 0] = [b_{ix}\ b_{iy}\ b_{iz}] \\ \mathbf{p}_i &= [r_p \cos(\Psi_i)\ r_p \sin(\Psi_i)\ 0] = [p_{ix}\ p_{iy}\ p_{iz}] \end{aligned} \quad (1)$$

where

$$\begin{aligned} \psi_i &= \frac{i\pi}{3} - \frac{\phi_b}{2} & \Psi_i &= \frac{i\pi}{3} - \frac{\phi_p}{2} & i &= 1,3,5 \\ \psi_i &= \psi_{i-1} + \phi_b & \Psi_i &= \Psi_{i-1} + \phi_p & i &= 2,4,6 \end{aligned}$$

The Stewart-Gough manipulator geometry was defined with two coplanar sets of vectors: $\mathbf{b}$ and $\mathbf{p}$; $\mathbf{b}$ corresponds to the fixed base and $\mathbf{p}$ to the movable platform (Lara-Molina et al., 2011). According to Eq. (1), the Stewart-Gough mechanism can be defined by five structure design parameters: r_b is the radius of the fixed base, r_p is the radius of the movable platform, ϕ_b is the spacing angle of the vectors $\mathbf{b}_i$, ϕ_p is the spacing angle of the vectors $\mathbf{p}_i$. Finally, s sets the length of the lower member as function of total length of the leg, thus the length of the upper member is defined as $h_{d_i} = s.l_i$ and the length of the lower member is $h_{u_i} = (1-s)l_i$. Consequently, the structure of mechanism can be parametrized by the vector $\boldsymbol{\lambda}_s \in \mathbb{R}^{5\times1}$.

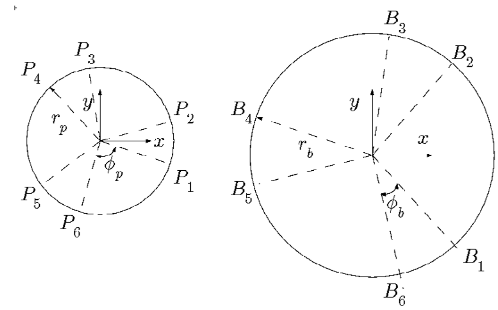

Fig. 2. Fixed base and movable platform.

$$\boldsymbol{\lambda}_s = [r_p\ \phi_p\ r_b\ \phi_b\ s]^T \quad (2)$$

2.2 Dynamic Model

The dynamic equations for the 6-UPS Stewart-Gough manipulator were derived in closed form through the Newton-Euler approach by (Dasgupta and Mruthyunjaya, 1998).

$$\mathbf{f} = \mathbf{J}^{-1}\mathbf{M}(\mathbf{q})\mathbf{J}^{-T}\ddot{\mathbf{q}} + \mathbf{J}^{-1}[\boldsymbol{\eta}(\mathbf{q}, \dot{\mathbf{q}}) - \mathbf{M}(\mathbf{q})\mathbf{J}^{-T}\mathbf{u}] \quad (3)$$

where,

- $\mathbf{f} = [f_1\ \ldots\ f_6]^T \in \mathbb{R}^{6\times1}$ is the actuator force vector.
- $\mathbf{J} = \begin{bmatrix} \mathbf{s}_1 & \ldots & \mathbf{s}_6 \\ \mathbf{p}_1 \times \mathbf{s}_1 & \ldots & \mathbf{p}_6 \times \mathbf{s}_6 \end{bmatrix} \in \mathbb{R}^{6\times6}$ is the Jacobian matrix. $\mathbf{s}_i$ is the unit vector along each leg, for $i = 1, \ldots, 6$ (Fig. 1).
- $\mathbf{q} = [l_1\ \ldots\ l_6]^T \in \mathbb{R}^{6\times1}$ is the leg length vector.
- $\dot{\mathbf{q}} = [\dot{l}_1\ \ldots\ \dot{l}_6]^T \in \mathbb{R}^{6\times1}$ is the leg velocity vector.
- $\ddot{\mathbf{q}} = [\ddot{l}_1\ \ldots\ \ddot{l}_6]^T \in \mathbb{R}^{6\times1}$ is the leg acceleration vector.
- $\mathbf{M} = \mathbf{M}_p + \sum_{i=1}^{6} \mathbf{M}_{li} \in \mathbb{R}^{6\times6}$ is the total inertia matrix which considers the inertia of the legs and the movable platform. This term includes the mass of the platform m_p.
- $\boldsymbol{\eta} = \boldsymbol{\eta}_{plat} + \sum_{i=1}^{6} \boldsymbol{\eta}_i \in \mathbb{R}^{6\times1}$ is the Coriolis, gravitation, centrifuge force vector of the movable platform and each leg, and viscous friction forces at the joints for the 6-UPS where c_u, c_p, c_s are the coefficients of viscous friction in the universal, prismatic and spherical joints, respectively.
- $\mathbf{u} \in \mathbb{R}^{6\times1}$ is an expression related to the acceleration of the legs.

Additional details of the formulation of the dynamic equations can be obtained in (Dasgupta and Mruthyunjaya, 1998).

The inertial properties of the movable platform and the six legs are defined as function of the structure parameters of Eq. (2). The geometric shape of the rigid bodies of the Stewart-Gough mechanism is defined as cylinders (see

Fig. 1). The inertia matrix and center of mass are defined based on the structure parameters $\boldsymbol{\lambda}_s$ and the density of each rigid body. The center of mass of the movable platform is attached to the coordinate frame $\{P\}$. The inertia matrix of the lower and upper members of the legs is defined with respect to the coordinate frames $\{U\}$ and $\{D\}$ (Fig. 1) and the centers of mass are $\mathbf{r}_{u_i} = [-h_{u_i}/2\ 0\ 0]^T$ and $\mathbf{r}_{d_i} = [h_{d_i}/2\ 0\ 0]^T$, respectively. The following parameters should be defined in order to describe the inertia of all rigid bodies as function of the structural parameters $\boldsymbol{\lambda}_s$: thickness of the movable platform h_p, radius of the upper r_u and lower r_l members of the legs, density of the material of the movable platform ρ_p and legs ρ_l.

2.3 Tracking position control

Computed Torque Control (CTC) is composed of two independent loops: an inner-loop to linearize the non-linear dynamic of the robot by means of the feedback linearization and an outer-loop to track a desired trajectory. Thus, the non-linear dynamic equation of the robot (Eq. (3)) can be written in a simplified way:

$$\mathbf{f}_c = \mathbf{A}(\mathbf{q})\ddot{\mathbf{q}} + \mathbf{h}(\mathbf{q}, \dot{\mathbf{q}}) \tag{4}$$

where $\mathbf{A}(\mathbf{q}) = \mathbf{J}^{-1}\mathbf{M}(\mathbf{q})\mathbf{J}^{-T}$ and $\mathbf{h}(\mathbf{q}, \dot{\mathbf{q}}) = \mathbf{J}^{-1}[\boldsymbol{\eta}(\mathbf{q}, \dot{\mathbf{q}}) - \boldsymbol{M}(\mathbf{q})\mathbf{J}^{-T}\mathbf{u}]$.

The robot equations can be linearized and decoupled by non-linear feedback. $\hat{\mathbf{A}}(\mathbf{q})$ and $\hat{\mathbf{h}}(\mathbf{q}, \dot{\mathbf{q}})$ are respectively the estimates of $\mathbf{A}(\mathbf{q})$ and $\mathbf{h}(\mathbf{q}, \dot{\mathbf{q}})$. Assuming that:

$$\begin{aligned} \hat{\mathbf{A}}(\mathbf{q}) &= \mathbf{A}(\mathbf{q}) \\ \hat{\mathbf{h}}(\mathbf{q}, \dot{\mathbf{q}}) &= \mathbf{h}(\mathbf{q}, \dot{\mathbf{q}}) \end{aligned} \tag{5}$$

the problem is reduced to a n linear and decoupled double-integrators system, where n is the number of degrees of freedom of the robot (i.e. n=6 in the considered application).

$$\ddot{\mathbf{q}} = \mathbf{w}_c \tag{6}$$

with $\mathbf{w}_c$ being the new input control vector. Equation (6) corresponds to the inverse dynamic control scheme, where the dynamic of the robot is transformed into a set of double integrators (see Fig. 3).

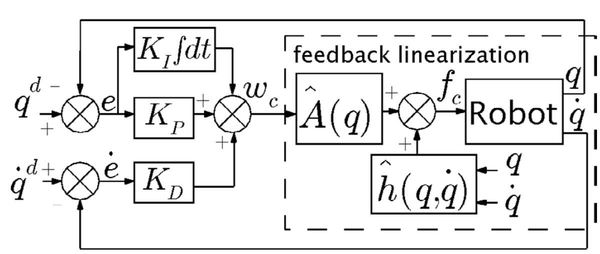

Fig. 3. The computed torque and PID, block diagram.

Assuming a PID controller on each joint one has:

$$\mathbf{w}_c = \mathbf{K}_P(\mathbf{q}^d - \mathbf{q}) + \mathbf{K}_D(\dot{\mathbf{q}}^d - \dot{\mathbf{q}}) + \mathbf{K}_I \int (\mathbf{q}^d - \mathbf{q})dt \tag{7}$$

The controller gains are $\mathbf{K}_P = diag(k_{P_1}, \ldots, k_{P_6})$, $\mathbf{K}_D = diag(k_{d_1}, \ldots, k_{d_6})$ and $\mathbf{K}_I = diag(k_{I_1}, \ldots, k_{I_6})$. The controller gains are tuned in order to have in continuous-time domain the following closed-loop characteristic equation for each decoupled double-integrator of Eq. 6: $(s+\omega_r)(s^2 + 2\xi\omega_r s + \omega_r^2) = 0$, where s is the Laplace variable. Thus, $k_P = (1 + 2\xi)\omega_r^2$, $k_D = (1 + 2\xi)\omega_r$, $k_I = \omega_r^3$.

For the tracking position control scheme shown in Fig. 3, it was assumed in Eq. (5) that the estimated and real terms are equal. Experimentally, this assumption is not valid due to the existence of unknown or uncertain parameters, e.g. friction parameters. Moreover, the robot manipulator should operate within a given range of payload values. In this way, it is necessary to analyze the effects of uncertain parameters on the closed-loop dynamics of the robot system, which includes both the mechanism and the control system.

3. STOCHASTIC ANALYSIS

Typically the inertial, friction and geometrical parameters of parallel robot are affected by uncertainties. The inertial and friction parameters should be identified to compute the model-based position controller; therefore estimated values with small error are introduced in the control algorithms. Manufacturing tolerances include small variations in the geometrical parameters (Paccot et al., 2009). Therefore, the parameters selected in order to introduce the uncertainties in the model presented in the previous section are: the structural parameters (r_p, ϕ_p, r_b, ϕ_b, s), the mass of the movable platform (m_p), and the viscous frictions of the joints (c_s, c_p, c_u).

The uncertain parameters are modeled as random variables. The corresponding uncertainties are introduced by using the relation:

$$a_0(\theta) = a_0 + a_0\delta_a\xi(\theta) \tag{8}$$

where a_0 is the mean value of the parameter, δ_a is the dispersion level and $\xi(\theta)$ is the unite normal random variable with θ being a random process. The unite normal random variable is governed by a normal distribution, this distribution was selected in order to evaluate the uncertain parameters in this contribution.

The so-called Monte Carlo method combined with the Latin Hypercube sampling (Florian, 1992) is used to simulate the dynamic response of the robot with the considered uncertain random parameters. Additionally, with the aid of a convergence analysis helps determining the number of Monte Carlo samples n_s to obtain an accurate result in the simulations.

4. SENSITIVITY ANALYSIS

The previous sections presented the robot modeling. The sensitivity analysis aims at determining the influence of each structure parameter and dynamic parameter on the dynamic response of the robot, specifically in terms of the variation of the position accuracy of the robot. Consequently, this analysis allows to indicate the degree of influence of each parameter on the variation of the position accuracy of the robot.

Among the various methods used to analyze the sensitivity, the variance-based sensitivity analysis decomposes the variance of the output of the model into fractions which are associated with the variation of each parameter (Saltelli et al., 2008). This method allows to quantify the effect of the variation of an individual parameter on the dynamic response of the robot by means of a probabilistic framework based on the Monte Carlo Simulation method. Additionally, this method copes with nonlinear models, which is suitable to quantify the sensitivity of the parallel robot.

Considering the model under the form $y = f(\mathbf{w})$, where y is a scalar output and $\mathbf{w} = [w_1 \ldots w_k]^T \in \mathbb{R}^{k\times 1}$ is a vector of k parameters. These parameters are considered as independently and uniformly distributed within the unit hypercube, i.e., $w_i \in [0,1]$ for $i = 1,\ldots,k$. $f(\mathbf{w})$ is decomposed:

$$y = f(\mathbf{w}) = f_0 + \sum_{i=1}^{k} f_i(w_i) + \sum_{i<j}^{k} f_{ij}(w_i,w_j) + \cdots + f_{12\ldots,k} \tag{9}$$

The decomposition of the variance expression is (Sobol', 1990):

$$V(y) = \sum_{i=1}^{k} V_i + \sum_{i<j}^{k} V_{ij} + \cdots + V_{12\ldots k} \tag{10}$$

where $V_i = V_{w_i}(E_{\mathbf{w}_{\sim i}}(y|w_i))$, $V_{ij} = V_{w_{ij}}(E_{\mathbf{w}_{\sim ij}}(y|w_{ij}))$, and so on. A variance based first order effect for a generic design parameter w_i is:

$$V_{w_i}(E_{\mathbf{w}_{\sim i}}(y|w_i)) \tag{11}$$

where w_i is the i-th parameter and $\mathbf{w}_{\sim i}$ denotes the matrix of all parameters except w_i. The meaning of the inner expectation operation is that the mean of y is taken over all possible values $\mathbf{w}_{\sim i}$ while keeping w_i fixed. The associated sensitivity measure denominated first-order sensitivity index is defined as:

$$s_i = \frac{V_{w_i}(E_{\mathbf{w}_{\sim i}}(y|w_i))}{V(y)} \tag{12}$$

s_i states the effect of the variation of w_i only, however divided by the variation in other parameters. Nevertheless, the total effect-index s_{Ti} measures the contribution to the output variance of w_i, including all the effects of its interactions with any other input parameter.

$$s_{Ti} = \frac{E_{\mathbf{w}_{\sim i}}(V_{w_i}(y|w_{\sim i}))}{V(y)} = 1 - \frac{V_{\mathbf{w}_{\sim i}}(E_{w_i}(y|w_{\sim i}))}{V(y)} \tag{13}$$

The Monte Carlo Simulation combined with the Latin Hypercube sampling (Florian, 1992) is used to calculate the total-effect indices. The total number of model evaluation to compute the total-sensitivity index is $N = n_s(k+1)$, where n_s is the number of the Monte Carlo samples (Saltelli et al., 2008).

5. SIMULATION RESULTS

The controlled robot model of Fig. 3 was used in the numerical simulation that was implemented in matlab/simulink. The values of structural and dynamical parameters of the parallel robot are given in table 1.

In order to analyze the effect of uncertainties in the position accuracy of the robot, small variations in some parameters around their nominal values are introduced in the model as presented in Eq. (8). Table 2 gives percentage of the dispersion level with respect to the mean value of each uncertain parameter considered in the model.

Two reference trajectories in the workspaces were considered in the analysis. First, a circular trajectory is implemented with translational motion of the movable platform in $x-y-z$ axis (Fig. 4). The second trajectory consists in a pure rotational motion of the movable platform around the $x-y-z$ axis with fixed position. It is worth mentioning that although the workspace trajectories are different, there is an equivalence in the maximum velocities in the joint space.

5.1 Uncertainty analysis

In the sequence, the convergence of the response variability with respect to the number of samples (n_s) used in the Monte Carlo simulation is verified, thus n_s=195.

For the circular trajectory, Fig. 4 shows the reference and the trajectories performed with the uncertain parameters. As seen, the uncertainties in the parameters produce a small variation in the trajectory tracked by the movable platform; consequently this variation increases the position error.

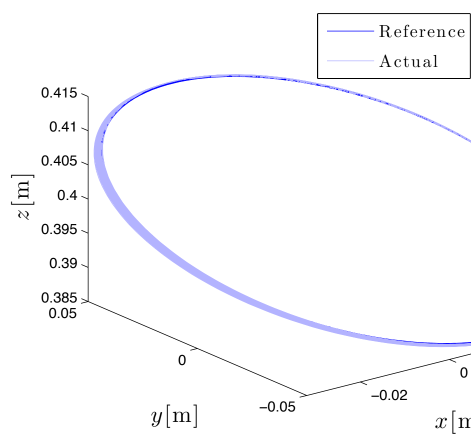

Fig. 4. Circular workspace trajectory, reference and uncertain trajectory.

In order to analyze the relationship between the position error and the velocity of the reference trajectory the Root

Table 1. Parameters of the robot.

Parameter	Mean value	Parameter	Mean value
r_p(m)	0.24	$r_{leg_u}(m)$	0.03
$\phi_p(^o)$	110	$r_{leg_d}(m)$	0.03
r_b(m)	0.29	ρ_p(kg/m^3)	2697
ϕ_b $(^o)$	32	ρ_l(kg/m^3)	7874
s	0.5	$h_p(m)$	0.01
c_u(Ns/m)	0.1	k_P	19200
c_p (Ns/m)	0.1	k_D	240
c_s (Ns/m)	0.2	k_I	512000

Table 2. Uncertain Parameters and dispersion levels.

Parameter	Dispersion level	Parameter	Dispersion level
r_p	0.1%	ϕ_p	0.1%
r_b	0.1%	ϕ_b	0.1%
s	0.1%	m_p	2%
c_u	10%	c_p	10%
c_s	10%		

Mean Square of the position joint-space error ($RMSE$) is evaluated for a determined range of velocities.

$$RMSE(\mathbf{e}) = \frac{1}{6}\sum_{i=1}^{6}\sqrt{e_i^T e_i} \qquad (14)$$

Fig. 5 presents the envelopes of random $RMSE$ as function of the maximum velocity (V_{max}) of the circular trajectory. The mean and the dispersion of the random $RMSE$ increases in accordance with the increasing of V_{max}. This indicates that the effect of uncertainties has a significant influence in high velocities.

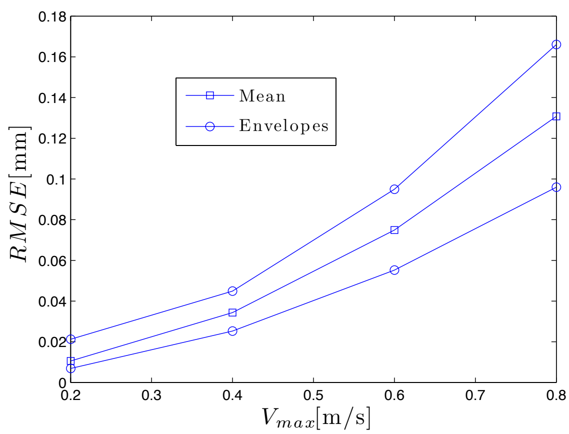

Fig. 5. Envelopes of random $RMSE$ as function of V_{max}.

Additionally, Fig. 6 shows the random force of the legs over the motion along the circular trajectory. A considerable variation in the force produced by the uncertain parameters is observed, e.g. at the instant t=0.47s the force of the first leg (f_{c_1}) has a percentage variation of 31% with respect to its mean instantaneous value. As seen, the variation in the force applied by the controller to each leg is not negligible and it should be considered in the design of the control system.

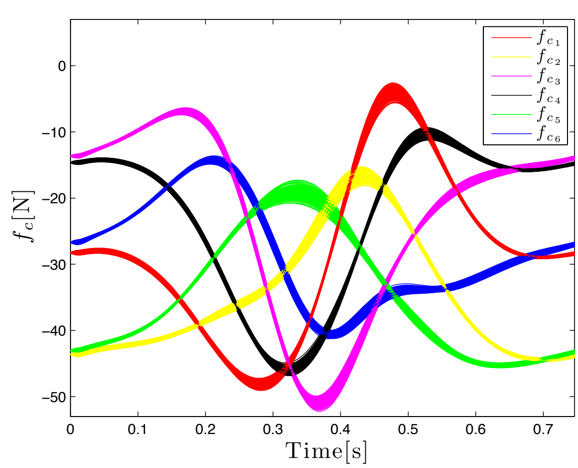

Fig. 6. Random force of the legs ($\mathbf{f}_c$), circular trajectory.

For the rotational trajectory, the uncertain analysis of the random $RMSE$ was also performed for a range of velocities showed in Fig. 7. Following the tendency of the previous uncertainty analysis, the mean and the dispersion of the random $RMSE$ increases with the increase of the rotational velocity of the movable platform. Nevertheless, in this case the dispersion of the random $RMSE$ is smaller.

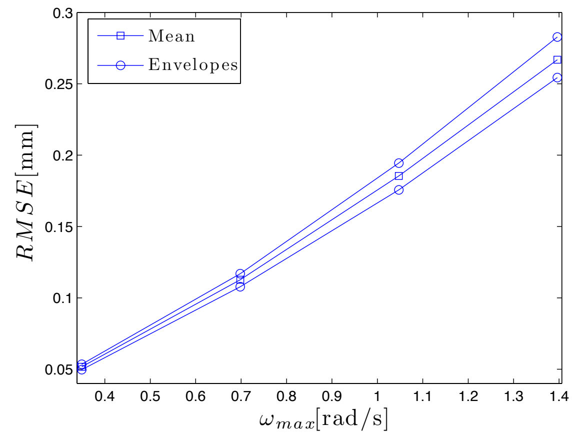

Fig. 7. Envelopes of random $RMSE$ as a function of ω_{max}.

5.2 Sensitivity Analysis

The sensitivity analysis was performed over the circular and rotational workspace trajectories used in the previous analysis with the maximum velocity respectively, however any other trajectory could be considered. The total effect-indices of the uncertain parameters of table 2 are computed by using the variance-based sensitivity analysis presented in section 4.

The number of computation of samples the Monte Carlo computation required to perform the sensitivity analysis was fixed at n_s=195 to ensure an accurate solution according to the convergence analysis. Considering k=9 variables, the total number of model evaluations is N=1950.

The total effect-indices of the uncertain parameters for the circular trajectory are showed in Fig. 8. As seen, the position accuracy is more sensitive to the mass of the platform m_p than the other variables. This is expected since the circular trajectory provides a translational motion of the movable platform, which influences the position accuracy with an uncertain m_p. However, among the uncertain parameters the structural parameters exhibit a significant sensitivity. For this trajectory, the uncertain friction force of the passive and active joints of the legs have a negligible sensitivity.

The total effect-indices of uncertain parameters for rotational trajectory are showed in Fig. 9. For this trajectory, the position accuracy is highly sensitive to the structural parameters of the parallel robot. The radius of the fixed base, the spacing angles of the movable platform and fixed base show a considerable sensitivity taking into account the fact that these parameters introduce small position errors between the actual and the position computed by the model based controller. The uncertain coefficients of the viscous friction of the passive and active joints of the legs are little sensitive, hence the results obtained agree with experimental results in which the fiction of the passive joints is not considered in the identification and control of

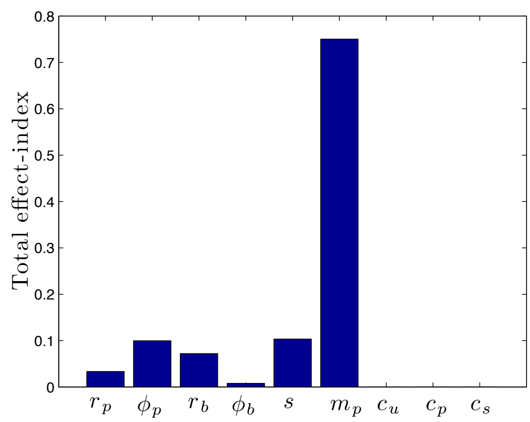

Fig. 8. Total effect-index, circular trajectory.

the parallel robots(Paccot et al., 2009; Lara-Molina et al., 2014b). The mass of the movable platform (m_p) has a small sensitivity since the position of the movable platform is constant.

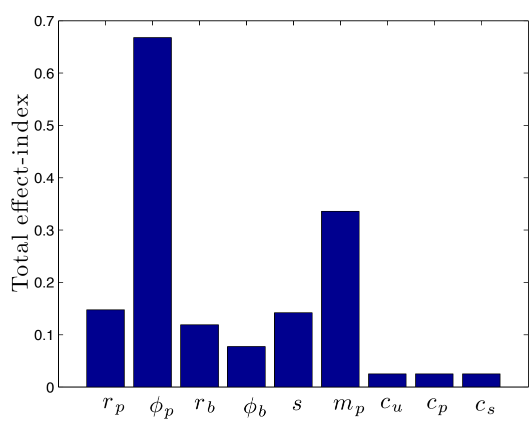

Fig. 9. Total effect-index, rotational trajectory.

6. CONCLUSION

In this contribution the effect of uncertain parameters on the dynamic behavior of a 6-DOF fully parallel robot was studied. Specifically, the PID computed torque was analyzed by considering uncertain structural and dynamic parameters. The simulation results indicate that the consideration of small parametric uncertainties in the numerical model of the parallel robot manipulator can affect significantly the dynamic behavior of the system in terms of position accuracy. Therefore, uncertain parameters should be taken into account in numerical simulation to obtain reliable numerical models for design purposes.

The stochastic analysis used in this contribution demonstrated to be a straightforward methodology to quantify the effect of uncertain parameters on the dynamic response of a parallel robot manipulator. Moreover, the sensitivity analysis allowed to determine the contribution of each uncertain parameter on the uncertain response of the robot. This is important to determine the degree of importance of the uncertain parameters on the dynamic response of the robot. Furthermore, the study of robot manipulator dynamics and control can be enhanced by the performance of uncertain analysis.

Further work will encompass the study of control techniques and design methods of parallel robots under uncertain parameters and dynamics.

ACKNOWLEDGEMENTS

The authors express their acknowledgements to the National Institute of Science and Technology of Smart Structures in Engineering (INCT-EIE), jointly funded by CNPq, CAPES and FAPEMIG.

REFERENCES

Dasgupta, B. and Mruthyunjaya, T.S. (1998). Closed-form dynamic equations of the general stewart platform through the Newton-Euler approach. *Mechanism and Machine Theory*, 33(7), 993–1012.

Florian, A. (1992). An efficient sampling scheme: updated latin hypercube sampling. *Probabilistic engineering mechanics*, 7(2), 123–130.

Kim, J., Song, W.J., and Kang, B.S. (2010). Stochastic approach to kinematic reliability of open-loop mechanism with dimensional tolerance. *Applied Mathematical Modelling*, 34, 1225–1237.

Lara-Molina, F., Koroishi, E., and Steffen, V. (2014a). Uncertainty analysis of a two-link robot manipulator under fuzzy parameters. In *Robotics: SBR-LARS Robotics Symposium and Robocontrol (SBR LARS Robocontrol), 2014 Joint Conference on*, 1–6.

Lara-Molina, F.A., Rosário, J.M., and Dumur, D. (2011). Multi-objective optimization of stewart-gough manipulator using global indices. In *Advanced Intelligent Mechatronics (AIM), 2011 IEEE/ASME International Conference on*, 79–85.

Lara-Molina, F.A., Rosário, J.M., Dumur, D., and Wenger, P. (2014b). Robust generalized predictive control of the orthoglide robot. *Industrial Robot: An International Journal*, 41(3), 275 – 285.

Merlet, J.P. (2009). Interval analysis and reliability in robotics. *Int. J. Reliability and Safety*, 3(1/2/3), 104–130.

Paccot, F., Andreff, N., and Martinet, P. (2009). A review on the dynamic control of parallel kinematic machines: Theory and experiments. *The International Journal of Robotics Research*, 28(3), 395–416.

Pandey, M.D. and Zhang, X. (2012). System reliability analysis of the robotic manipulator with random joint clearances. *Mechanism and Machine Theory*, 58, 137–152.

Saltelli, A., Ratto, M., Andres, T., Campolongo, F., Cariboni, J., Gatelli, D., Saisana, M., and Tarantola, S. (2008). *Global Sensitivity Analysis: The Primer*. John Wiley & Sons Chichester, England.

Sobol', I.M. (1990). On sensitivity estimation for nonlinear mathematical models. *Matematicheskoe Modelirovanie*, 2(1), 112–118.

Voglewede, P., Smith, A.H.C., and Monti, A. (2009). Dynamic performance of a scara robot manipulator with uncertainty using polynomial chaos theory. *IEEE Transactions on Robotics*, 25(1), 206–210.